Comparative Study of Various Slot Pitches for 2-Pole 6-Slot Ultra-high-Speed Permanent Magnet Synchronous Motors

Jae-Hyun Kim[1], So-Yeon Im[2], Soo-Min An[2], Kyoung-Soo Cha[1], and Myung-Seop Lim[1]

[1]Department of Automotive Engineering, Hanyang University, Seoul 04763, Republic of Korea
[2]Department of Automotive Engineering (Automotive-Computer Convergence), Hanyang University, Seoul 04763, Republic of Korea

The 2-pole 6-slot (2p6s) permanent magnet synchronous motor (PMSM) is an attractive option for ultra-high-speed (UHS) applications due to its excellent manufacturability and balanced magnetic force. UHS PMSMs should be designed with short stack lengths and end coil heights to address rotor dynamics issues. In addition, given their high frequency, these PMSMs should be designed considering stator iron loss, rotor eddy current loss, and ac copper loss. The performance of the same pole-slot combination varies significantly based on the slot pitch. Hence, we compared the size and efficiency of the 2p6s UHS PMSM based on the slot pitch. For a fair comparison, an optimal design was performed for each slot pitch. To reduce computation time, optimization was conducted in two stages: size minimization and efficiency maximization. It was confirmed that in terms of total axial length, the one-slot pitch UHS PMSM is the shortest due to the advantage of having a short-end coil height, even with the lowest winding factor and largest stack length. Furthermore, it was determined that the two-slot pitch UHS PMSM offers an excellent trade-off between efficiency and size.

Index Terms— **Efficiency, end coil height, optimization, slot pitch, ultra-high-speed (UHS) motor.**

I. Introduction

ULTRA-HIGH-SPEED (UHS) permanent magnet synchronous motors (PMSMs) have attracted increasing interest in recent years due to their compact size and high power density [1]. These motors offer the advantages of compact size, high power density, and lightweight construction. However, there are important considerations in the design of UHS PMSMs. First, a rotor design that considers critical speed is necessary [2]. If the rotor rotates at a bending critical speed, then it can mechanically fail. The critical speed increases as the diameter of the rotor increases and the axial length of the rotor decreases. However, given that the rotor of a UHS PMSM is generally designed considering mechanical stress, there is a limit to increasing the rotor diameter. Therefore, to minimize the axial length of the rotor, it is essential to reduce the stack length of the stator and the height of the end coil to minimize the size of the UHS PMSM packaging size. Second, given that the UHS PMSM operates at high frequencies, it is necessary to design the motor considering stator iron loss, rotor eddy current loss, and ac copper loss [3], [4].

The stack length, end coil height, and efficiency of the motor are significantly affected by the number of poles and slots and the winding configuration. However, it is challenging to change the number of poles because UHS PMSMs are primarily designed with two-pole configurations by considering the switching frequency [5]. In addition, distributed windings with more than 12 slots exhibit poor manufacturability and high-end coil height. For a two-pole three-slot motor, large vibrations can occur due to an unbalanced magnetic force [6]. Given these considerations, the 2-pole 6-slot (2p6s) UHS PMSM is an attractive option for UHS PMSM. In [7], the performance of 2p6s UHS PMSM according to end winding configuration was investigated, but the performance according to slot pitch was not analyzed. In [8], the performances according to the slot pitch of a 2p6s UHS PMSM were compared. However, the models compared in [8] were optimized to maximize the torque for different power specifications. In practice, it is necessary to compare the performances of motors with the same input power, considering inverter specifications.

Therefore, in this study, 2p6s UHS PMSMs with slot pitches of 1–3 were optimized under the same power specifications and output power, and their sizes and efficiencies were compared. In Section II, a winding factor and end coil height of 2p6s PMSM according to slot pitch are analyzed. In Section III, the optimum design of UHS PMSM for each slot pitch was performed for a fair comparison. In addition, the performance of optimized UHS PMSM for each slot pitch was compared. Subsequently, in Section IV, a prototype of the two-slot pitch 2p6s UHS PMSM was fabricated, and the simulation results were validated by the test results.

II. Motor Topologies

Fig. 1 shows the winding configuration of the 2p6s PMSM according to the slot pitch. The stack length and end coil height of the PMSM varies significantly based on the slot pitch, and the stack length is dependent on the fundamental winding factor. Given that the distribution winding factor of the 2p6s PMSM is 1, the total winding factor is determined by the pitch factor, which can be expressed as follows:

$$k_{pn} = \sin\left(\frac{n\beta\pi}{2}\right) \tag{1}$$

Manuscript received 24 March 2023; revised 30 May 2023; accepted 1 June 2023. Date of publication 5 June 2023; date of current version 24 October 2023. Corresponding author: M.-S. Lim (e-mail: myungseop@hanyang.ac.kr).

Color versions of one or more figures in this article are available at https://doi.org/10.1109/TMAG.2023.3282741.

Digital Object Identifier 10.1109/TMAG.2023.3282741

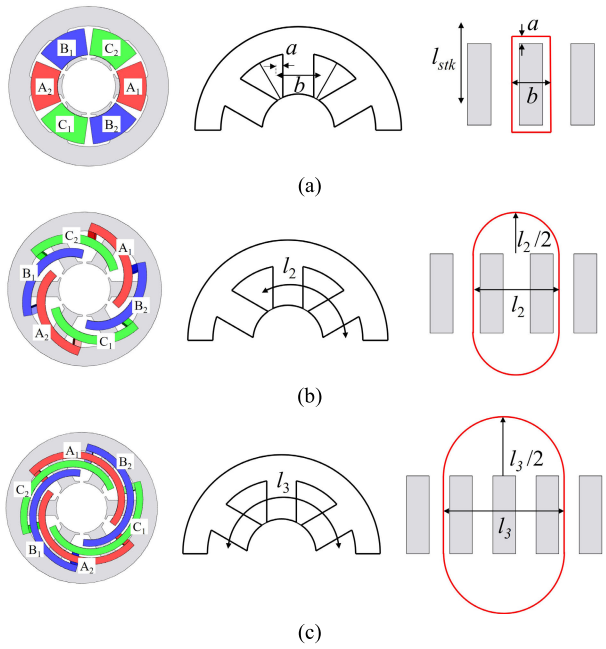

Fig. 1. Winding configuration of 2p6s PMSM according to slot pitch. (a) One-pitch. (b) Two-pitch. (c) Three-pitch.

TABLE I
TARGET SPECIFICATIONS

Parameters	Value	Unit
Maximum stator diameter	115.0	mm
Maximum rotational speed	110	krpm
Current density	8.5	A_{rms}/mm^2
Slot fill factor	60.0	%
DC link voltage	1.0	p.u.
Fundamental phase voltage limit	0.548	p.u.

where k_{pn} denotes the pitch factor of nth harmonic, n denotes the harmonic order, and $\beta\pi$ denotes the slot pitch in radian. Then, the fundamental winding factors of the 1-, 2-, and 3-slot pitch were calculated to be 0.5, 0.866, and 1.0, respectively. The stack length of the three-slot pitch can be designed to be the shortest under the same output torque conditions because a high fundamental winding factor is advantageous for torque generation.

However, given that the packaging size of the motor is determined by the sum of the stack length and end coil height, the end coil height is analytically calculated according to the slot pitch. For simplicity, the end coil configuration is assumed to be rectangular in the case of a one-pitch model as shown in Fig. 1(a). For two- and three-pitches, the end coil is assumed to have a semicircular shape as shown in Fig. 1(b) and (c). Then, the one-pitch end coil height is determined as $2a$, which is twice the distance between the tooth and center of the half-slot, and the end coil heights of two- and three-pitches are as follows:

$$l_{\text{end},i} = \frac{i\pi}{3}\left(\frac{R_{s\_o} - t_y + R_{s\_i} + t_{\text{tip}}}{2}\right) \ (i = 2, 3) \qquad (2)$$

where i denotes the slot pitch, R_{s_o} denotes the outer stator radius, t_y denotes the yoke thickness, R_{s_i} denotes the inner stator radius, and t_{tip} denotes the tooth tip thickness.

III. Optimal Design Process and Results

The optimization for each slot pitch was carried out to analyze the performances of each slot pitch of the UHS PMSM. The target specifications of the UHS PMSM are summarized in Table I. The rotor was designed to maximize the no-load air-gap magnetic flux density while considering mechanical stress. The optimal design was performed in two steps to reduce computation time as shown in Fig. 2: size minimization and efficiency maximization [9]. To calculate efficiency, a 3-D finite element analysis (FEA) is essential for calculating rotor eddy current loss, which significantly increases computation time. Therefore, to reduce computation time, 2-D FEA was used for size minimization, and 3-D FEA was utilized for efficiency maximization.

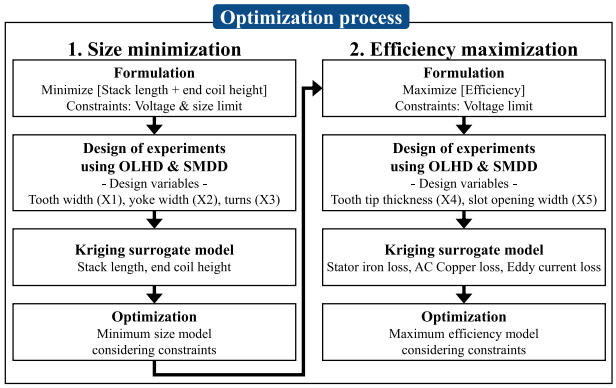

Fig. 2. Optimization process: size minimization and efficiency maximization.

TABLE II
LOWER AND UPPER BOUNDARIES FOR SIZE MINIMIZATION

Design variables	1-pitch		2-pitch		3-pitch	
	Lower	Upper	Lower	Upper	Lower	Upper
Tooth width (mm)	2	12	2	12	2	12
Yoke width (mm)	6	20	6	20	6	20
Series turns	35	45	22	26	19	23

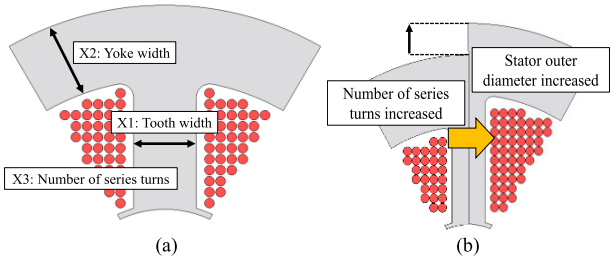

Fig. 3. Design variables for size minimization. (a) Design variables. (b) Configuration of PMSM according to number of turns.

A. Optimal Design for Size Minimization

The total axial length of the UHS PMSM, which is the sum of the stack length and end coil height, was minimized for each slot pitch. The reluctance of the main magnetic flux path is primarily determined by the tooth and yoke thicknesses, and the stack length varies significantly according to the number of series turns under the same current conditions. Therefore, the tooth and yoke thicknesses and the number of series turns per phase were determined as design variables for size minimization, as shown in Fig. 3(a). Here, the coil diameter is fixed considering the maximum current density condition. The upper and lower boundaries of the design variables are summarized in Table II. The lower and upper boundaries of the number of series turns per phase were determined by considering the winding factor for each slot pitch. The optimal Latin

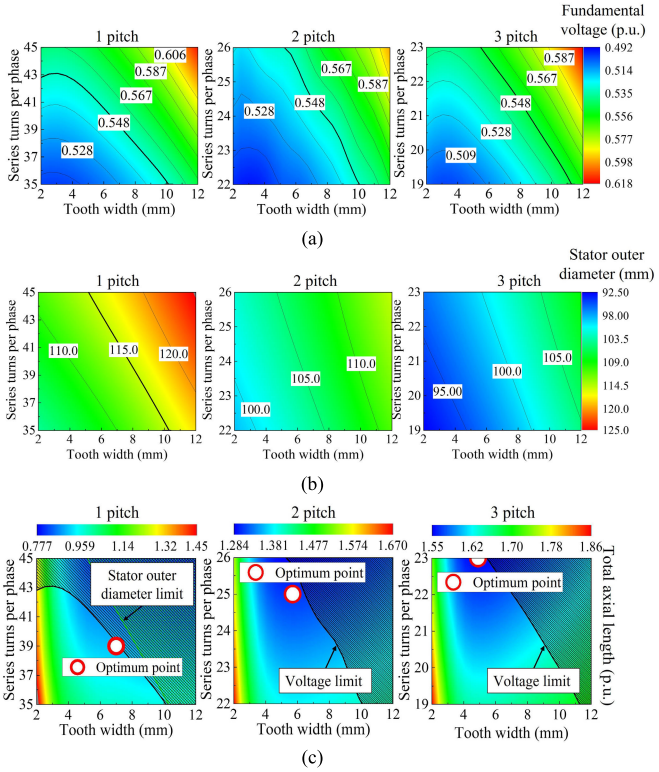

Fig. 4. Kriging surrogate model and size minimization optimum point. (a) Fundamental voltage. (b) Stator outer diameter. (c) Total axial length and optimum point.

TABLE III
LOWER AND UPPER BOUNDARIES FOR EFFICIENCY MAXIMIZATION

Design variables	1-pitch		2-pitch		3-pitch	
	Lower	Upper	Lower	Upper	Lower	Upper
Slot opening width	2 mm	7 mm	3 mm	7 mm	3 mm	7 mm
Tooth tip thickness	0.5 mm	2.5 mm	0.5 mm	2.5 mm	0.5 mm	2.5 mm

hypercube design (OLHD) and sequence maximin distance design (SMDD) were utilized for the design of experiments. The Kriging surrogate models for the main performance are shown in Fig. 4. The fundamental voltage trends shown in Fig. 4(a) according to the tooth width and the number of series turns are similar for 1-, 2-, and 3-slot pitches. Since the coil diameter is fixed, as the number of series turns increases, the slot area increases as shown in Fig. 3(b). Accordingly, the yoke inner radius and stator outer diameter increase as the slot pitch decreases, as shown in Fig. 4(b). As explained in Figs. 1 and (2), the end coil height increases as the slot pitch increases. Thus, the total axial length of the UHS PMSM tends to increase with the slot pitch as shown in Fig. 4(c).

For the optimization method, sequential quadratic programming (SQP) is utilized, and the optimization problem is expressed as follows:

$$\begin{aligned} &\text{minimize} L_{\text{stk}} + L_{\text{end}} \\ &\text{subject to} V_{\text{fund}} \le V_{\text{fund\_limit}}, \ D_s \le D_{s\_\text{limit}}, \ T = T_{\text{target}} \end{aligned} \quad (3)$$

where L_{stk} and L_{end} are the stack length and end coil height, respectively, V_{fund} is the fundamental induced voltage, D_{s} is the stator outer diameter, and T is the torque. Optimized models that minimize the total axial length while satisfying the voltage and stator outer diameter constraints were determined for each slot pitch, as shown in Fig. 4(c).

TABLE IV
DESIGN PARAMETERS AND PERFORMANCES OF OPTIMIZED MODELS

Parameters	1-pitch	2-pitch	3-pitch
Stack length (p.u.)	1.31	1.00	0.92
End coil height (p.u.)	0.44	1.04	1.52
Stator total axial length (p.u.)	**1.75**	**2.04**	**2.45**
Stator outer diameter (mm)	113.4	105.2	99.2
Tooth / Yoke width (mm)	7.0 / 15.9	5.7 / 18.6	4.9 / 16.9
Tooth tip thickness (mm)	0.9	1.15	1.07
Slot opening width (mm)	2.0	3.0	3.0
Number of series turns per phase	39	25	23
Core iron loss (W)	318.4	249.6	239.9
Rotor eddy current loss (W)	336.5	288.1	268.0
AC copper loss (W)	505.9	363.3	388.4
Efficiency (%)	**95.56**	**96.52**	**96.54**

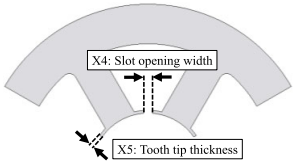

Fig. 5. Design variables for efficiency maximization.

B. Optimal Design for Efficiency Maximization

In calculating the efficiency, the iron loss of the stator and rotor core, eddy current loss of the PM and sleeve, and ac copper loss occurring in the stator windings, were considered. The slot opening width is strongly correlated with the eddy current loss because it determines the air-gap permeance. In addition, given that the tooth tip thickness and slot opening width are related to the slot leakage flux, they have a strong correlation with iron loss and ac copper loss. Therefore, the slot opening width and tooth tip thickness are determined as design variables for efficiency maximization, as shown in Fig. 5. The upper and lower boundaries of the design variables are summarized in Table III. For one-slot pitch UHS PMSM, the lower boundary of the slot opening width was determined to be 2 mm because it can be manufactured with a segmented stator, whereas those of the two- and three-slot pitch UHS PMSMs were determined to be 3 mm. The Kriging surrogate models for the losses and efficiency are shown in Fig. 6. Since the iron loss is proportional to the volume of the stator core for the same frequency and magnetic flux density, iron loss of the one-slot pitch UHS PMSM is the largest due to its large stator outer diameter and stack length as shown in Fig. 6(a). As the slot opening width decreased and the tooth tip thickness increased, the stator iron loss increased. This is because the slot leakage reluctance through the tooth tip is reduced, leading to an increase in the magnetic flux flowing through the slot opening as shown in Fig. 7. Since the rotor eddy current loss is proportional to the volume of the sleeve and PM, it decreases as the slot pitch increases as shown in Fig. 6(b). The rotor eddy current loss increased with the slot opening width. Given that the time-varying magnetic flux density in the rotor is mainly caused by the permeance variance of the stator, the smaller the slot opening width, the smaller the eddy current loss. Fig. 8 shows the rotor magnetic flux density waveform according to the slot opening width, which indicates that the time-varying magnetic flux density is smaller when the slot opening width is smaller. The ac copper loss is proportional to the ac resistance. Since the one-slot pitch UHS PMSM has the largest number

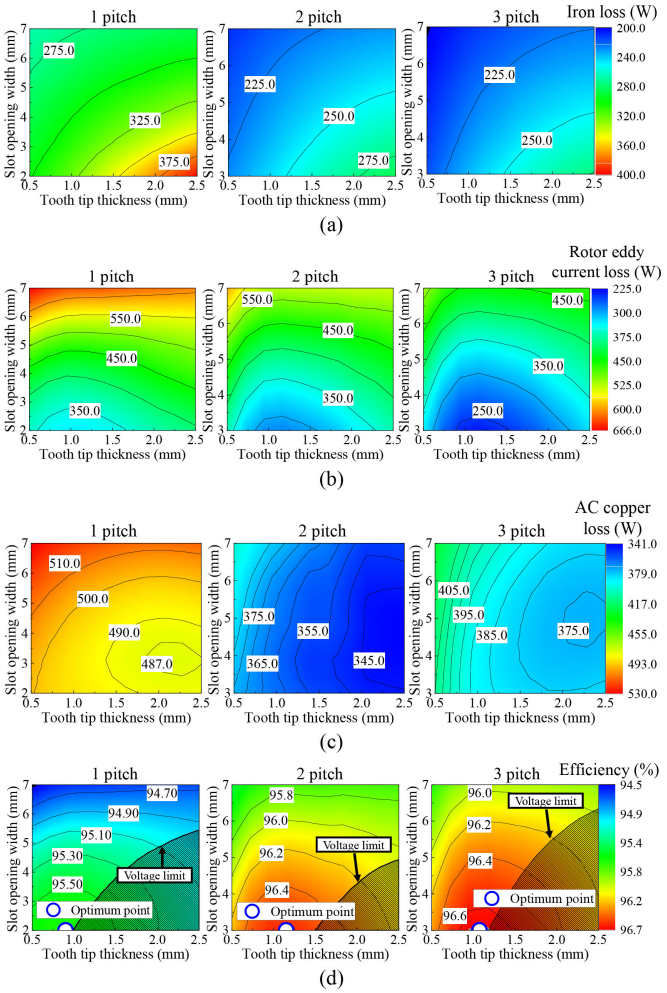

Fig. 6. Kriging surrogate model and efficiency minimization optimum point. (a) Iron loss. (b) Rotor eddy current loss. (c) AC copper loss. (d) Efficiency.

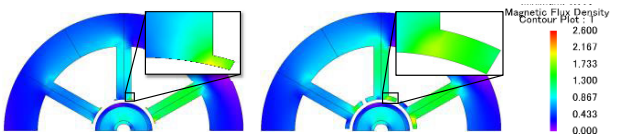

Fig. 7. Magnetic flux density contour of 2p6s one-slot pitch UHS PMSM according to slot opening width and tooth tip thickness.

of series turns, it also has the largest ac resistance due to its longest total coil length. Therefore, the ac copper loss of the one-slot pitch UHS PMSM is the largest as shown in Fig. 6(c). The number of turns of two- and three-slot pitch PMSM is similar, but the end coil height of three-slot pitch PMSM is almost 1.5 times longer than that of two-slot pitch PMSM as explained in Fig. 1 and (2). Therefore, the ac resistance and copper loss of three-slot pitch PMSM is larger than two-slot pitch PMSM as shown in Fig. 6(c).

The efficiency maximization optimal design was performed using SQP, and the optimization problem can be expressed as follows:

$$\begin{aligned} &\text{maximize}\eta \\ &\text{subject to}V_{\text{fund}} \le V_{\text{fund\_limit}}\,,\ T = T_{\text{target}} \end{aligned} \tag{4}$$

where η denotes the efficiency. The optimized models that maximized efficiency while satisfying the voltage constraint were determined for each slot pitch, as shown in Fig. 6(d).

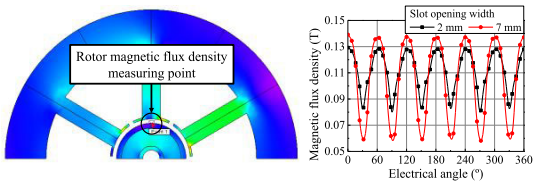

Fig. 8. Rotor time-varying magnetic flux density of 2p6s one-slot pitch UHS PMSM according to slot opening width.

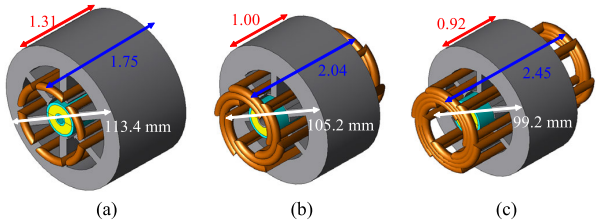

Fig. 9. Configurations of the optimized models. (a) One-slot pitch. (b) Two-slot pitch. (c) Three-slot pitch.

C. Performance Comparison With Respect to Slot Pitch

The parameters and performance of the optimized models for each slot pitch are summarized in Table IV, and their configurations are shown in Fig. 9. As presented in Table IV, as the slot pitch increases, the stack length of the UHS PMSM decreases. However, the total axial length increased as the height of the end coil increased. The number of series turns per phase of the one-slot pitch UHS PMSM was larger than that of the other slot pitch UHS PMSMs owing to its low winding factor; thus, the copper loss was relatively large. In addition, the rotor eddy current loss and stator iron loss were high owing to the long stack length; therefore, it can be observed that the efficiency of the one-slot pitch UHS PMSM is the lowest. Overall, the 2p6s one-slot pitch UHS PMSM exhibited the shortest overall axial length including the end coil height, but also the lowest efficiency. Conversely, the two-slot pitch UHS PMSM exhibits an excellent tradeoff relationship between axial length and efficiency. However, it was confirmed that the three-slot pitch UHS PMSM exhibits the longest axial length, but has almost no advantage when compared to the two-slot pitch in terms of efficiency.

IV. Validation

A prototype of the optimized 2p6s two-slot pitch UHS PMSM was fabricated and verified via tests. Fig. 10 shows the stator and compressor assembly of the 2p6s two-slot pitch UHS PMSM prototype. It can be observed that the ratio of the theoretically predicted stack length and total axial length (1:2.04) was almost similar to that of the actually manufactured prototype (1:2.10).

A no-load test was conducted to confirm that the prototype was manufactured correctly. Fig. 11(a) shows the no-load test setup, and Fig. 11(b) shows the measured and simulated back electro-motive force (BEMF) results. The test was conducted by rotating the servo motor at 1000 r/min. The relative error of the BEMF fundamental wave was 3.1%, which is acceptable.

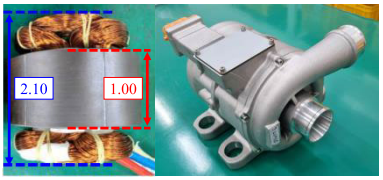

(a) (b)

Fig. 10. Prototype of the 2p6s two-slot pitch UHS PMSM. (a) Stator. (b) Air compressor assembly.

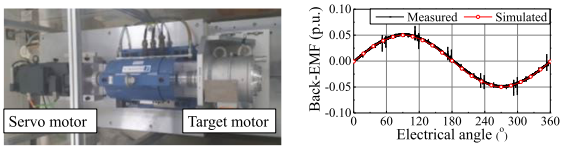

(a) (b)

Fig. 11. No-load test setup and results. (a) Test setup. (b) BEMF.

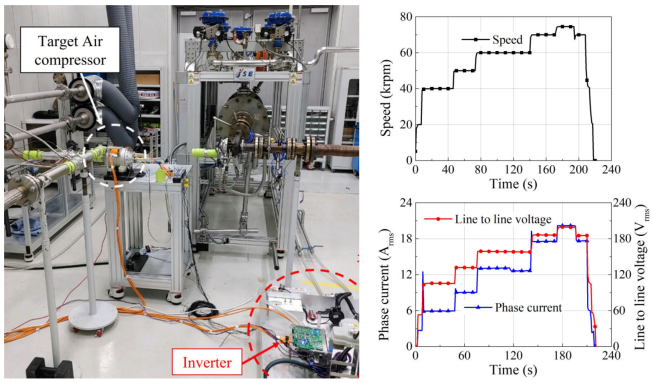

(a) (b)

Fig. 12. Air compressor system test setup and results. (a) Test setup. (b) Test results.

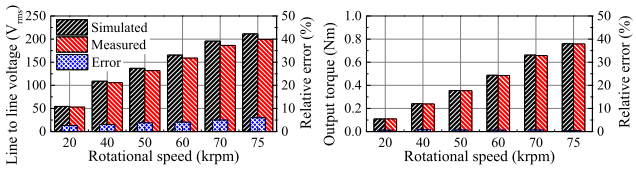

(a) (b)

Fig. 13. Simulated and measured results. (a) Line-to-line induced voltage. (b) Output torque.

Subsequently, an air compressor system test was conducted. Fig. 12 shows the air compressor system test setup and test results. Given that it is practically difficult to prepare a torque sensor and servo motor that can operate at a UHS of 110 kr/min, an air compressor system test was performed instead of a dynamometer test. As the voltage limit of the dc power supply was insufficient to operate at a maximum speed of 110 kr/min, the test was performed at a maximum speed of 75 kr/min. Fig. 13 shows the measured and 3-D simulated results of the induced voltage and torque according to the rotational speed. The torque was indirectly estimated by using the following method. The BEMF constant is calculated using the BEMF obtained from the no-load test as shown in Fig. 11. The torque constant was then calculated using the relationship between the torque constant and BEMF constant. Finally, the output torque is estimated by multiplying the phase current, which is measured using an oscilloscope in the air compressor system test as shown in Fig. 12, with the torque constant. As shown in Fig. 13, the relative errors of measured and simulated induced voltage and torque were within 6% and 0.7%, respectively, which is agreeable.

V. Conclusion

In this study, the performance of 2p6s UHS PMSMs was analyzed and compared with respect to slot pitch. To ensure a fair comparison, each slot pitch UHS PMSM was optimized in the same manner. To reduce computation time, optimization was performed in two stages: size minimization and efficiency maximization. The optimization revealed that the total axial length including the end coil height of one-slot pitch UHS PMSM was the shortest, even with the longest stack length. The two- and three-slot pitch UHS PMSMs exhibit longer end coil lengths; therefore, their total axial lengths are longer than that of the one-slot pitch UHS PMSM. However, owing to the high winding factor, the efficiencies of the two- and three-slot pitch UHS PMSMs were higher than that of the one-slot pitch UHS PMSM. Among them, the two- and three-slot pitch UHS PMSMs showed almost no differences in efficiency. Therefore, it was determined that the two-slot pitch UHS PMSM exhibits an excellent trade-off relationship in terms of the total axial length and efficiency, and the one-slot pitch UHS PMSM has an advantage in terms of the total axial length. Finally, a prototype of the optimized two-slot pitch UHS PMSM was fabricated, and the analysis results were verified via no-load and air compressor system tests.

Acknowledgment

This work was supported by the Ministry of Trade, Industry and Energy/Korea Evaluation Institute of Industrial Technology through the Research and Development Program under Grant 20010986.

References

[1] G. Gallicchio et al., "Surface permanent magnet synchronous machines: High speed design and limits," *IEEE Trans. Energy Convers.*, vol. 38, no. 2, pp. 1311–1324, Jun. 2022.

[2] Z. Huang and Y. Le, "Rotordynamics modelling and analysis of high-speed permanent magnet electrical machine rotors," *IET Electr. Power Appl.*, vol. 12, no. 8, pp. 1104–1109, Sep. 2018.

[3] J. Kim, D. Kim, Y. Jung, and M. Lim, "Design of ultra-high-speed motor for FCEV air compressor considering mechanical properties of rotor materials," *IEEE Trans. Energy Convers.*, vol. 36, no. 4, pp. 2850–2860, Dec. 2021.

[4] D. Kim, J. Kim, S. Lee, M. Park, G. Lee, and M. Lim, "Estimation method for rotor eddy current loss in ultrahigh-speed surface-mounted permanent magnet synchronous motor," *IEEE Trans. Magn.*, vol. 57, no. 2, pp. 1–5, Feb. 2021.

[5] A. Farhan, M. Johnson, K. Hanson, and E. L. Severson, "Design of an ultra-high speed bearingless motor for significant rated power," in *Proc. IEEE Energy Convers. Congr. Expo. (ECCE)*, Detroit, MI, USA, Oct. 2020, pp. 246–253.

[6] J. Ma and Z. Q. Zhu, "Mitigation of unbalanced magnetic force in a PM machine with asymmetric winding by inserting auxiliary slots," *IEEE Trans. Ind. Appl.*, vol. 54, no. 5, pp. 4133–4146, Sep./Oct. 2018.

[7] T. He, Z. Q. Zhu, F. Xu, Y. Wang, H. Bin, and L. Gong, "Electromagnetic performance analysis of 6-slot/2-pole high-speed permanent magnet motors with coil-pitch of two slot-pitches," *IEEE Trans. Energy Convers.*, vol. 37, no. 2, pp. 1335–1345, Jun. 2022.

[8] T. R. He et al., "Comparative study of 6-slot/2-pole high-speed permanent magnet motors with different winding configurations," *IEEE Trans. Ind. Appl.*, vol. 57, no. 6, pp. 5864–5875, Aug. 2021.

[9] S. Im, S. Lee, D. Kim, G. Xu, S. Shin, and M. Lim, "Kriging surrogate model-based design of an ultra-high-speed surface-mounted permanent-magnet synchronous motor considering stator iron loss and rotor eddy current loss," *IEEE Trans. Magn.*, vol. 58, no. 2, pp. 1–5, Feb. 2022.